Phonon propagation in nonpolar semiconductor heterostructures

Fernando de León-Pérez[1,2] and Rolando Pérez-Alvarez[1]
[1]*Physics Faculty, Havana University 10400 Havana, Cuba*
[2]*Physics Department, Central University ''Marta Abreu'' of Las Villas, Santa Clara, Cuba*
(Received 11 July 2000; revised manuscript received 12 December 2000; published 29 May 2001)

A recently developed long-wavelength continuum phenomenological model is employed to study phonon tunneling for an arbitrary incidence angle, and to estimate the contribution of optical phonons to the perpendicular thermal conductivity in simple and multisuperlattice nonpolar semiconductor heterostructures. Phonon tunneling is a multicomponent problem with different tunneling channels. We rigorously define the transmission and reflection coefficients from the energy density balance equation. Simple general rules are presented for the relationship between (a) the key features of the transmission and reflection rates, and (b) the vibrational properties. The range of applicability of the model is increased by simultaneously considering both acoustic and optical phonons. The defined coefficients are employed to test the interrelationship between the coupled modes. Interesting oscillation effects in the relative contribution of different coefficients as a function of the incidence angle are found. We report numerical results for isotopic Ge superlattices to illustrate the model considered. Approximate analytical expressions for the dispersion relation are derived for this system. The contribution of optical phonons to the thermal conductivity is elucidated with the help of these expressions.

DOI: 10.1103/PhysRevB.63.245304 PACS number(s): 63.22.+m, 68.65.−k, 66.70.+f

I. INTRODUCTION

The vibrational characteristics of multilayered structures are of both fundamental and practical interest. Optical spectroscopies are suitable for the investigation of semiconductor microstructures, and can also be used to characterize the quality of the heterostructures, in particular the details of the interfaces (for a review, see Ref. 1). In order to explain the main experimental results, different models have been developed to describe the phonon dispersion curves. These models range from simplified linear chain models[2] to the most elaborate ones based on *ab initio* local-density calculations.[3] Most optical spectroscopies are subject to rather stringent selection rules which arise from wave-vector conservation. In fact, the phonon created or annihilated must have a wave vector of magnitude close to zero, i.e., near the center of the Brillouin zone. For this reason, phenomenological long-wavelength models are successful when compared with experimental results.

It is interesting to note the preference of theoreticians for long-wavelength models to study acoustic[4,5] and optical[6,7] phonons. These approaches can accommodate the symmetry of the materials, if desired. Compared with other phenomenological and *ab initio* models, these help to visualize the physics of the problems, due to the comparative reduction in the computational effort, and to the predominantly analytical nature of the study.

Recently, a phenomenological continuum approach was developed for polar optical oscillations in semiconductor nanostructures.[7–9] It simultaneously satisfies mechanical and electrostatic matching conditions, and has been applied successfully to double heterostructures, superlattices (SL's) and quantum dots.[8,10] A detailed presentation of this model can also be seen in Ref. 9. In the spirit of this approach, we proposed a continuum model for nonpolar optical phonons, and obtained it formally as a coupling constant between mechanical oscillations and the electric field vanishes, as expected for nonpolar crystals.[11] Details of this model, and a calculation of eigenvalues and eigenmodes in different nonpolar heterostructures, considering real interfaces, were presented in this reference. The model[7] contains Christoffel equations for acoustic phonons[12] as a particular case, with the right selection of the input parameters. In the present paper we study both acoustic and optical vibrations in nonpolar materials, employing the long-wavelength approach.[11] We show that the model for optical phonons is a counterpart of that corresponding to acoustic phonons; considering both together, the best results compared with other methods and experimental data are obtained. We focus on the propagation of phonons through finite simple and multisuperlattice structures.

Acoustic-phonon tunneling has been intensively studied, both theoretically with Christoffel equations[4,5] and experimentally with phonon imaging.[13] Employing a long-wavelength model for phonon tunneling, Ridley elucidated the electrostatic character of the vibrational modes in one barrier polar heterostructure.[6] Phonon tunneling in nonpolar systems is analyzed in the present paper. It is a multicomponent problem with different tunneling channels. The transmission and reflection coefficients are rigorously defined from the energy density balance equation, which is derived without approximations. To the best of our knowledge, these analytical results have not been discussed even for the well-studied acoustic phonons (see, for example, Ref. 4 for acoustic phonons and Ref. 6 for optical phonons). Elimination of the electrostatic coupling simplifies the formulation of the problem, which can then be carried out analytically. The phonon normal incidence (a one-dimensional problem) allows for a complete analytical treatment, and is a generalization of the results for acoustic phonons of Mizuno and Tamura.[5]

One of the purposes of the present work is to explain how phonon tunneling describes all the features of the vibrational modes in semiconductor heterostructures. We present some simple rules to show the equivalence between this approach and the usual numerical diagonalization. Also, the interrelation between the coupled modes is tested.

The recently observed reduction of thermal conductivity both in-plane[14] and perpendicular to the interface[15] in semiconductor superlattices, compared with the values in bulk materials, implies a potentially attractive application for heterostructures in thermoelectronic devices.[16] Hyldgaard and Mahan[17] showed that the thermal conductivity of a SL is reduced because the phonon group velocity is decreased relative to its value in the bulk constituents (among other reasons presented in Refs. 15 and 18). To analyze these problems, Hyldgaard and Mahan and Tamura *et al.*[19] employed simple lattice models that took account of the acoustic phonons. Very recently, more realistic full three-dimensional (3D) calculations began to appear,[20,21] and showed that the simple previous approaches explain the main qualitative features of this physical problem and offer good quantitative estimations, even at high temperatures.

The most drastic reduction of the thermal conductivity occurs at high temperatures (>100 K), when the peak in the Planck phonon distribution is at frequencies characteristic of optical phonons, e.g., at $T=257$ K, and $\omega=502$ cm^{-1} (The peak in the number of phonons per unit frequency is given by $\hbar\omega=2.8k_BT$). We recall that, due to the rather flat nature of the optical-phonon branches, the corresponding group velocity is very small. Therefore, the weight of optical phonons in heat transfer may be small even at high temperatures. A different behavior is expected for the materials studied below, where an important contribution of the optical phonons is found.

Regarding the propagation of thermal energy through crystalline solids, we note that at low temperature the principal source of thermal conduction are the acoustic phonons in the GHz (10^9 Hz) to THz (10^{12} Hz) range. At room temperature the propagation of thermal phonons is highly diffusive, with mean free paths resulting from phonon scattering. This limits the optical-phonon imaging.

The most suitable systems to study phonon transmission are isotopic Ge SL's. An isotopic Ge SL refers to two layers of enriched Ge isotopes repeated periodically. These systems were investigated intensively in the last years.[22,23] The phonon-dispersion relations of two isotopically enriched Ge bulk materials overlap over a large frequency range. This allows phonon SL bands to be more dispersive, which implies larger absolute values of the group velocity perpendicular to the growth direction in layered structures, and consequently a greater contribution of the optical phonons to the thermal transport and transmission peaks, broader and better resolvable with numerical methods than in Si/Ge structures. Also, strain effects are not important. These features are stimulating for an experimental study. Another interesting system is the Si/Ge SL. The physics of phonon tunneling is about the same. A short report of numerical results for normal incidence only was presented elsewhere.[24]

For the sake of completeness, we summarize the main features of the long-wavelength model relevant to this paper in Sec. II, and present general analytical properties, i.e., the derivation of the energy density balance equation, and some approximations which are useful for isotopic SL's. In Sec. III the main analytical properties of the phonon tunneling are described with the help of a transfer-matrix method, and the results of the preceeding Sec. II. In Sec. IV we present numerical results for different Ge SL's. We first study the simple periodic superlattice to show how we can explain the phonon physics through the transmission rate. Then we analyze multiple superlattices as an example of the usefulness of the model in more complex systems. The oblique incidence of phonons is discussed later. We consider the contribution of optical phonons to thermal conductivity in Sec. V. Finally some conclusions are given.

II. LONG-WAVELENGTH MODEL

We first analyze the optical phonons. For a description of the oscillations we use the displacement vector field **u**, which represents the relative displacement of the two atoms in the unit cell. Other physical parameters of the medium are $\rho=\overline{M}/v_c$, the reduced mass density, where $\overline{M}$ is the reduced mass of the atoms and v_c the unit-cell volume; ω_T and ω_L are the limiting longitudinal (L) and transverse (T) bulk frequencies; β_T and β_L are two parameters describing the dispersion of the oscillations, i.e., for bulk materials the L and T branches have the parabolic behavior $\omega_{L,T}^2(\mathbf{k})=\omega_{L,T}^2-\beta_{L,T}^2k^2$ in the neighborhood of the Γ point of the Brillouin zone. In layered structures all these quantities are piecewise constants, and are dependent on the coordinates.

All the following results are valid for acoustic phonons if the vector field **u** now represents the atomic center-of-mass displacements. We should also make the replacement $\beta_{L(T)}^2\rightarrow-\beta_{L(T)}^2$ [$\beta_{L(T)}$ is the $L(T)$ sound velocity], where $\omega_{L(T)}=0$, and the reduced mass is substituted for by the total mass of the cell. In this way the Christoffel equations of motion and, in particular, the linear dispersion relation for the bulk $\omega_{L(T)}=\beta_{L(T)}k$, are obtained. For simplicity, in the rest of the paper we shall limit ourselves to writing formulas for optical vibrations.

In the spirit of the theory of continuous media, we postulate the Hamiltonian density

$$\mathcal{H}=\frac{1}{2}\rho\left|\frac{\partial\mathbf{u}}{\partial t}\right|^2+\frac{1}{2}\rho\omega_T^2|\mathbf{u}|^2+\frac{\sigma_{ij}u_{ji}^*+\sigma_{ji}^*u_{ij}}{4}. \qquad (1)$$

The first term is the kinetic-energy density, and the second term represents the coupling of the displacement field **u** with itself. The last term incorporates the internal stresses of the medium, and leads to the dispersive character of the oscillations. $\boldsymbol{\sigma}$ is the ''stress'' tensor, first defined in Ref. 7, which takes into account the symmetry properties of the medium. By standard procedures the following system of coupled second-order differential equations (equations of motion) are obtained:

$$\rho\frac{\partial^2\mathbf{u}}{\partial t^2}=-\rho\omega_T^2\mathbf{u}+\boldsymbol{\nabla}\cdot\boldsymbol{\sigma}. \tag{2}$$

To obtain the continuity equation for the energy density, we first integrate, in the volume of the whole space, the scalar product of the temporal derivative of **u** times the equation of motion (2); then we take the Hermitian conjugates in the resulting equation, and add both together. Integrating by parts and after a straightforward algebra, we find the energy density balance equation

$$\frac{\partial\mathcal{H}}{\partial t}+\boldsymbol{\nabla}\cdot\mathbf{j}=0, \tag{3}$$

where the energy density flux is given by

$$\mathbf{j}=-\frac{1}{2}\left(\frac{\partial\mathbf{u}^\dagger}{\partial t}\cdot\boldsymbol{\sigma}+\frac{\partial\mathbf{u}}{\partial t}\cdot\boldsymbol{\sigma}^\dagger\right). \tag{4}$$

As in Ref. 11, in order to study the materials considered here, it suffices to study the case of cubic symmetry. In layered structures, we Fourier transform in the layer planes, which introduces a 2D wave vector $\boldsymbol{\kappa}$, and we are thus left with a differential system in z, the normal coordinate. In this case, after assuming harmonic solutions and solving the equation of motion (2), we find the solution space

$$u_x(y,z,t)=ik_T(B_T^te^{ik_Tz}-B_T^re^{-ik_Tz})e^{i(\kappa y-\omega t)}, \tag{5}$$

$$\begin{vmatrix}u_y(y,z,t)\\u_z(y,z,t)\end{vmatrix}=\left(A_L^t\begin{vmatrix}i\kappa\\ik_L\end{vmatrix}e^{ik_Lz}+A_L^r\begin{vmatrix}i\kappa\\-ik_L\end{vmatrix}e^{-ik_Lz}\right)e^{i(\kappa y-\omega t)}+\left(A_T^t\begin{vmatrix}-ik_T\\i\kappa\end{vmatrix}e^{ik_Tz}+A_T^r\begin{vmatrix}ik_{Tj}\\i\kappa\end{vmatrix}e^{-ik_Tz}\right)e^{i(\kappa y-\omega t)}, \tag{6}$$

where

$$k_{L(T)}=\sqrt{\frac{\omega_{L(T)}^2(\Gamma)-\omega^2}{\beta_{L(T)}^2}-\kappa^2}, \tag{7}$$

and the transverse wave vector $\boldsymbol{\kappa}$ is assumed without lost of generality in the y direction due to the isotropy of the media.[11] For convenience the solutions are written as traveling waves. The subscript $L(T)$ labels the longitudinal (transverse) independent solutions. The superscript $t(r)$ labels the wave moving to the right (left), which we shall call a transmitted (reflected) wave when studying the phonon tunneling. The transverse horizontal solution [Eq. (5)] is decoupled from the oscillations in the directions y and z [Eq. (6)]. For $\boldsymbol{\kappa}=0$ the solution space is decoupled into purely longitudinal and doubly degenerate transverse vibrations.

The secular equation for the coupled modes can be written in the matrix form[11]

$$\det\begin{pmatrix}A & \kappa B\\ \kappa C & D\end{pmatrix}=0. \tag{8}$$

The order of the submatrices A, B, C, and D depends on the problem under consideration (2×2 in the quantum-well case and 4×4 in the SL case). The diagonal submatrix $A(D)$ contains only transverse (longitudinal) magnitudes for $\boldsymbol{\kappa}=0$. On the other hand the nondiagonal submatrices C and B are responsible for the L-T mixing for $\boldsymbol{\kappa}\neq0$.

On studying numerically isotopic superlattices, we find that for $\boldsymbol{\kappa}\neq0$ the coupling between longitudinal and transverse solutions is not strong. In a first approximation we can neglect the off-diagonal terms in Eq. (8), and obtain a dispersion relation for a superlattice,

$$\cos(qd)=\cos(k_{L(T)w}l)\cos(k_{L(T)b}h)-\frac{1}{2}\left(\xi+\frac{1}{\xi}\right)\sin(k_{L(T)w}l)\sin(k_{L(T)b}h), \tag{9}$$

where

$$\xi=\frac{\rho_w\beta_{L(T)w}^2k_{L(T)w}}{\rho_b\beta_{L(T)b}^2k_{L(T)b}}; \tag{10}$$

q is the SL Bloch wave vector, and $d=l+h$ is the SL period. In the frequency range of forbidden propagation $k_{L(T)b}$ is imaginary. Note that the right-hand side of Eq. (9) is function of κ, and that the two transverse solutions are degenerate.

The fraction ξ is close to unity for most SL's. That is especially true for isotopic SL's due to the small changes in the parameters of the constituent materials. Setting $\xi=1$ as a zeroth-order approximation in Eq. (9), we find the condition for folded bulk dispersion curves (no gaps open):

$$k_{L(T)w}l+k_{L(T)b}h=qd+2\pi n,\quad n=0,\pm1,\pm2,\ldots. \tag{11}$$

From here it is straightforward to obtain an explicit relation for ω as a function of q and κ for each band n. This relation is not valid for confined states. In the limiting case the confined phonons are obtained from the condition $k_{L(T)w}l=n\pi/2$.[11] In the next-order approximation the width of the gaps [at frequency ω_n in Eq. (11), such that $qd=m\pi$] is found to be

$$\Delta\omega_n=\frac{\sqrt{2\gamma\sin(k_{L(T)w}^{(n)}l)\sin(k_{L(T)b}^{(n)}h)}}{\omega_n\left(\dfrac{l}{\beta_{L(T)w}k_{L(T)w}^{(n)}}+\dfrac{h}{\beta_{L(T)b}k_{L(T)b}^{(n)}}\right)}, \tag{12}$$

where $\gamma=(1-\xi)^2/2\xi$. For acoustic phonons at $\boldsymbol{\kappa}=0$ the result of Tamura *et al.*[4] is recovered.

In isotopic SL's the gaps are small, and we can employ the dispersion relation and phonon group velocity normal to the grow direction of the heterostructure derived from Eq. (11) to calculate the thermal conductivity. In this way we are considering both optical and acoustic modes in the whole reciprocal space within the approximation that the modes practically do not interact between them.

III. TUNNELING PROBLEM

In our problem we have three different channels for the phonon tunneling: two transverse channels and one longitudinal channel [Eqs. (5) and (6)]. Due to the fact that the transverse horizontal solution is decoupled from the other solutions, this channel is independent of the other two. However, this case remains interesting because the differences with respect to the one-dimensional one. Also, a simple analytical formulation is possible. To construct the associated transfer matrix, we introduce the column vector

$$W_j(z)=\begin{vmatrix}\mathbf{u}_j\\ \sigma_{jz}\end{vmatrix}, \tag{13}$$

where $\sigma_{jz}=\boldsymbol{\sigma}\cdot\hat{e}_j$, and $j=1$ and 2 label the well and barrier materials, respectively. Employing the solution space [Eqs. (5) and (6)], we can write $W_j(z)$ as

$$W_j(z)=h_j(z)C_j. \tag{14}$$

In particular, for the coupled solutions [Eq. (6)] we find (the TH modes and the limiting case of decoupled solutions for $\boldsymbol{\kappa}=0$ are discussed later)

$$h_j(z)=\begin{pmatrix} i\kappa e^{ik_{Lj}z} & i\kappa e^{-ik_{Lj}z} & -ik_{Tj}e^{ik_{Tj}z} & ik_{Tj}e^{-ik_{Tj}z}\\ ik_{Lj}e^{ik_{Lj}z} & -ik_{Lj}e^{-ik_{Lj}z} & i\kappa e^{ik_{Tj}z} & i\kappa e^{ik_{-Tj}z}\\ 2B_j\kappa k_{Lj}e^{ik_{Lj}z} & -2B_j\kappa k_{Lj}e^{-ik_{Lj}z} & E_j e^{ik_{Tj}z} & E_j e^{-ik_{Tj}z}\\ D_j e^{ik_{Lj}z} & D_j e^{-ik_{Lj}z} & 2B_j\kappa k_{Tj}e^{ik_{Tj}z} & -2B_j\kappa k_{Tj}e^{-ik_{Tj}z}\end{pmatrix}, \tag{15}$$

$$B_j=\rho_j\beta_{Tj}^2,\quad D_j=\rho_j[\kappa^2(\beta_{Lj}^2-2\beta_{Tj}^2)+\beta_{Lj}^2k_{Lj}^2],$$
$$E_j=\rho_j\beta_{Tj}^2(\kappa^2-k_{Tj}^2), \tag{16}$$

and

$$C_j=\begin{vmatrix}A_{Lj}^t\\ A_{Lj}^r\\ A_{Tj}^t\\ A_{Tj}^r\end{vmatrix}. \tag{17}$$

$A_{L(T)j}^t$ and $A_{L(T)j}^r$ are the longitudinal (transverse) transmitted (t) and reflected (r) oscillation amplitudes.

Returning to the general case of both TH and coupled solutions, let us consider the first layer A_1 between the substrate X and the second layer A_2. The boundary conditions demand that

$$W_{A_1}(0)=W_X(0),$$
$$W_{A_1}(d_{A_1})=W_{A_2}(d_{A_1}). \tag{18}$$

Employing Eqs. (14) and (18), we find

$$W_{A_2}(d_{A_1})=t_{A_1}(d_{A_1})W_X(0), \tag{19}$$

where

$$t_{A_1}(d_{A_1})=h_{A_1}(d_{A_1})h_{A_1}^{-1}(0). \tag{20}$$

In a similar way we can define the matrix t_{A_2} for the layer A_2:

$$t_{A_2}(d_{A_2})=h_{A_1}(d_{A_1}+d_{A_2})h_{A_1}^{-1}(d_{A_1}). \tag{21}$$

The transfer matrix for the SL is given by

$$T_{SL}=t_{A_2}t_{A_1}. \tag{22}$$

The transfer matrix for finite SL's with N periods is obtained after multiplying the transfer matrix for each individual SL, i.e., $T_{SL}(N)\equiv T_{SL}^N$.

The transmission and reflection coefficients are defined from the energy density balance equation. For the cubic ''stress'' tensor[11] and the associated solution space [Eqs. (5) and (6)], we have an explicit expression for the energy density flux [Eq. (4)] in the heterostructure growth direction z,

$$j_z=\rho_j\omega\beta_{Tj}^2k_{Tj}(|B_{Tj}'^t|^2-|B_{Tj}'^r|^2)+\rho_j\omega\beta_{Lj}^2k_{Lj}(|A_{Lj}'^t|^2-|A_{Lj}'^r|^2)$$
$$+\cdots+\rho_j\omega\beta_{Tj}^2k_{Tj}(|A_{Tj}'^t|^2-|A_{Tj}'^r|^2), \tag{23}$$

where the primed constants are related with the adimensional constants employed in the solution space [Eqs. (5) and (6)] in the following way:

$$\frac{|B_{Tj}'^t|^2}{|B_{Tj}^t|^2}=k_{Tj}^2,\quad \frac{|A_{Lj}'^t|^2}{|A_{Lj}^t|^2}=(k_{Lj}^2+\kappa^2),\quad \frac{|A_{Tj}'^t|^2}{|A_{Tj}^t|^2}=(k_{Tj}^2+\kappa^2). \tag{24}$$

The same holds for the reflected components. Note that there is no interference between the individual fluxes in Eq. (23), and that the flux for each component is equal to the product of the energy density $\rho_j\omega^2A_{L(T)j}^{t(r)}$ (or $\rho_j\omega^2B_{L(T)j}^{t(r)}$) times the group velocity $|\partial\omega/\partial\mathbf{k}|=\beta^2k/\omega$. We can define the transmission and reflection coefficients (rates) for the longitudinal and transverse modes $T_{L(T)}$ and $R_{L(T)}$, respectively, in the forms

$$T_T^x = \rho_j \omega \beta_{Tj}^2 k_{Tj} |B_{Tj}'^t|^2 / j_{zi}, \tag{25}$$

$$R_T^x = \rho_j \omega \beta_{Tj}^2 k_{Tj} |B_{Tj}'^r|^2 / j_{zi}, \tag{26}$$

$$T_L = \rho_j \omega \beta_{Lj}^2 k_{Lj} |A_{Lj}'^t|^2 / j_{zi}, \tag{27}$$

$$R_L = \rho_j \omega \beta_{Lj}^2 k_{Lj} |A_{Lj}'^r|^2 / j_{zi}, \tag{28}$$

$$T_T = \rho_j \omega \beta_{Tj}^2 k_{Tj} |A_{Tj}'^t|^2 / j_{zi}, \tag{29}$$

$$R_T = \rho_j \omega \beta_{Tj}^2 k_{Tj} |A_{Tj}'^r|^2 / j_{zi}. \tag{30}$$

The superscript x labels the transverse horizontal modes, and j_{zi} is the incident flux. The following relation between the fluxes holds for the defined coefficients:

$$T_T^x + R_T^x + T_L + R_L + T_T + R_T = 1. \tag{31}$$

Discarding the TH solutions for the moment, and focusing our attention on the coupled solutions, we relate the coefficients in the substrate X and detector Y with the help of Eq. (14):

$$\begin{vmatrix} A_{LY}^t \\ A_{LY}^r \\ A_{TY}^t \\ A_{TY}^r \end{vmatrix} = T \begin{vmatrix} A_{LX}^t \\ A_{LX}^r \\ A_{TX}^t \\ A_{TX}^r \end{vmatrix}. \tag{32}$$

T is the convenient product of matrices h_i and h_i^{-1} [Eqs. (20) and (21)], according to the number of blocks in the finite SL. For the tunneling boundary condition we have different possibilities. The simplest and most common situation is the incidence of a phonon, e.g., a longitudinal one, from the left side with amplitude $A_{LX}^t = 1$, in such a way that $A_{TX}^t = A_{LY}^r = A_{TY}^r = 0$. In the following we limit ourselves to this case.

To obtain expression (23), we assumed in the calculations that for $\kappa \neq 0$ the condition $\omega_L = \omega_T$ is fulfilled. This condition is valid for optical and acoustic phonons in unstrained materials. For a biaxial deformation the stress related to the mismatch leads to the splitting of the L and T phonon frequencies in the bulk materials ($\omega_L \neq \omega_T$). For strained materials are needed both a different ''stress'' tensor and the corresponding solution space to substitute in the expression for the energy density flux. For the strained Si/Ge structures studied in Ref. 24, expression (23) constitutes a good approximation (although the results are exact only for $\kappa = 0$).

The normal incidence can be obtained as the limiting case ($\kappa \to 0$) of the above expressions. For this 1D problem, a complete analytical development is possible. The theory of transmission of perpendicular acoustic phonons through a finite superlattice using a transfer matrix approach can be seen in Ref. 5. Defining the optical impedance as $\Upsilon_i = \rho_i \beta_i^2 k_i$, and employing the expression ζ defined in Ref. 5, the formulas valid for optical phonons can be easily obtained from Ref. 5, making the substitution $\Upsilon_i \to -\Upsilon_i$ and $\zeta \to -\zeta$.

Multiple-superlattice system

The above results can be easily generalized to structures as complex as required. In fact, the corresponding transfer matrix is obtained after multiplying the transfer matrix of each finite superlattice with N_i periods. The sequence could also be either a regular or a quasiregular one, e.g., following the Fibonacci sequence. As an example we apply analytical expressions for the transfer matrix in the normal incidence to a triple-superlattice structure, where it is still possible to obtain analytical results. The system we consider consists of finite superlattices *A*, *B*, and *A*, grown on a substrate. For phonons propagating through the *ABA* system, the relevant transfer matrix is

$$T_{ABA} = T_A(N) T_B(M) T_A(N). \tag{33}$$

The $A(B)$ SL has $N(M)$ periods. In the following the subscripts A and B denote the corresponding SL. The calculations of the matrix product of Eq. (33) is straightforward. The explicit expressions for T_{ABA} can be easily obtained from Ref. 5 with the same replacement that for the simple SL's. The resonance condition in the *ABA* multisuperlattice structures (G_+) discussed in Ref. 5 are also valid for optical phonons.

IV. PHONON TUNNELING IN ISOTOPIC GERMANIUM SUPERLATTICES

For the ^{70}Ge (^{74}Ge) atom we have used the same mass and the same value $\omega_{LO}(\Gamma) = \omega_{TO}(\Gamma) \approx 309(301)$ cm^{-1} of Ref. 23. As the isotopic composition is changed, the atomic vibration frequencies are mainly rescaled by the mass.[22] In this case the optical branches for bulk materials are shifted rigidly, and the parameters $\beta_L^2 \approx 2.83 \times 10^{-12}$ and $\beta_T^2 \approx 5.50 \times 10^{-12}$ for both isotopes coincide with the corresponding values of natural Ge; these are obtained by fitting the data from Ref. 25 to the curve of the bulk dispersion relations. For acoustic phonons, we obtain the parameters $\beta_L^2 \approx -5.61 \times 10^{-12}$ and $\beta_T^2 \approx -1.77 \times 10^{-12}$ in the same way for natural Ge, and rescale these by the isotope mass. We assume the simplest situation when both the substrate and detector are of the same material as the well, i.e., ^{70}Ge.

In Fig. 1 we compare the dispersion relation for an infinite SL in the direction [001], with the transmission coefficient for a perpendicular longitudinal phonon (T_L) calculated for a 20 barrier $(^{70}\text{Ge})_4$-$(^{74}\text{Ge})_4$ finite SL. Both acoustic and optical phonons are studied. A good agreement with other theoretical and experimental results is obtained.[22,23] For optical modes the agreement is excellent, while the acoustic branches have frequencies lower than expected. This is related to the input parameters we choose. We take the topmost (lowest) branches for the optical (acoustic) phonons. We choose the input parameters in order to guarantee that (a) the optical and acoustic branches do not overlap, and (b) that the number of modes for a value of q be equal to the number of degrees of freedom of the atoms in the supercell. In this sense, studying the optical and acoustic vibrations at the same time, we improve the results of the calculations. Note also that we obtain good results at the relatively large wave-

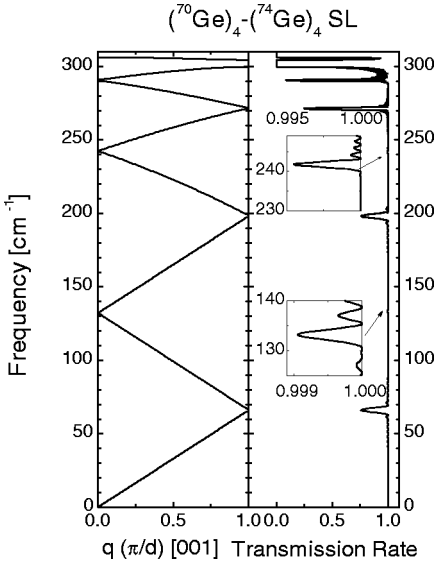

FIG. 1. Calculated LO-phonon dispersion curves (frequency in cm^{-1}) for an infinite (^{70}Ge)$_4$-(^{74}Ge)$_4$ SL along the [001] direction and transmission rate of a normal L phonon (T_L) for a 20-barrier SL. d is the SL period. Both optical and acoustic modes are presented. The length in the q axis is normalized to the unity.

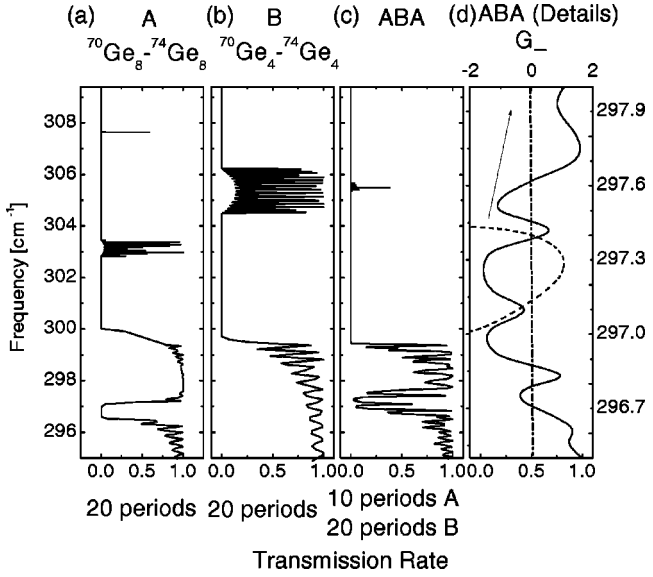

FIG. 2. Multiple-superlattice system (optical modes, normal incidence). (a) A is a 20 period (^{70}Ge)$_8$-(^{74}Ge)$_8$ SL, and (b) B is a 20 period (^{70}Ge)$_4$-(^{74}Ge)$_4$ SL. (c) The ABA system shows a resonance in the A dip. (d) The resonance condition G_- brought into coincidence with the transmission peaks. G_- is represented by a dashed line. See the text for details.

vector value $q=\pi/d$ (d is the SL period) compared to the length of the Brillouin zone of the massive crystal ($4\pi/d$).

A coincidence between the width of the transmission peak (dip) and the phonon bandwidth (gapwidth) is observed. Note that the gaps at the edge of the mini Brillouin zone are broader than at $q=0$, as expected from Eq. (12). As expected for an isotopic SL, the gaps between minibands are very small—practically indistinguishable on the scale of Fig. 1—and Eq. (11) is a good approximation. Some additional oscillations are present, originating from the interference effects in the finite SL. In general, it is found that the transmission dips in the continuum region are more pronounced at higher frequencies. For lower frequencies in the continuum the modes are more extended through the whole structure, and the transmission rate is closer to unity.

In the transmission rate we can also compare the different natures of the confined and folded phonon modes. The mode confined in ^{70}Ge shows a resonance peak. The more confined the phonon the narrower the peak, corresponding to flatter phonon branches (for larger SL periods the highest frequency phonons are more confined.[22,23]) The modes confined in ^{74}Ge, which penetrate significantly into the adjacent layers, and the modes extended through the SL present characteristic transmission dips at the gaps of the phonon spectra. In this way the transmission rate describes the features of the phonon modes.

The same features of simple superlattices remain valid for multisuperlattices and for arbitrary incidence angles, as discussed below. In this way we can elucidate the nature of the phonon modes in all kinds of structures. The even greater periodicity of the multisuperlattices introduces additional characteristics. As an example we study the case of a triple ABA multisuperlattice for perpendicular LO-phonon incidence. The results are presented in Figs. 2 and 3. In Fig. 2, the letter A labels a ten period (^{70}Ge)$_8-$(^{74}Ge)$_8$ SL, and B a 20-period (^{70}Ge)$_4$-(^{74}Ge)$_4$ SL. In the frequency interval (296,298) cm^{-1} some transmission dips appear in the A structure; conversely, in the B structure this interval corresponds to allowed states [see Figs. 2(a) and 2(b)]. In the ABA system some resonances appear in the A dip [Fig. 2(c)]. These are well explained by the resonance condition G_- generalized from Ref. 5, as shown in Fig. 2(d). The small deviation between frequency satisfying $G_-=0$ and the location of the transmission peak arises from the finite number ($N=10$) of periods assumed for superlattice A. As N be-

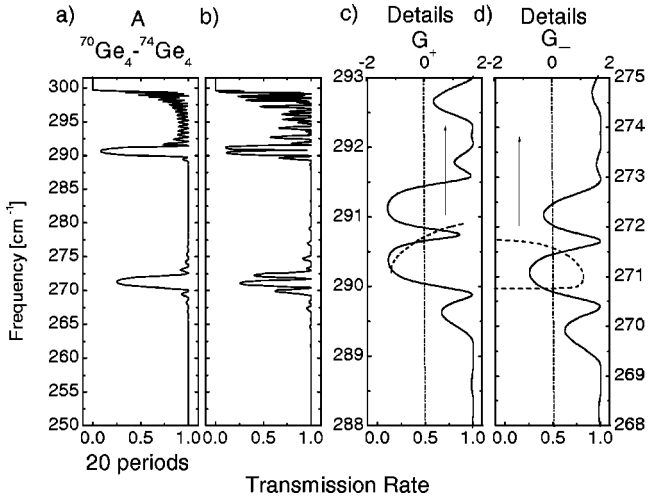

FIG. 3. Multiple-superlattice system (optical modes, normal incidence). (a) A is a 20-period (^{70}Ge)$_4$-(^{74}Ge)$_4$ SL, and (b) is an ABA SL; B represents 80 periods of bulk ^{70}Ge. G_+ (c) and G_- (d) are represented by dashed lines. See the text for details.

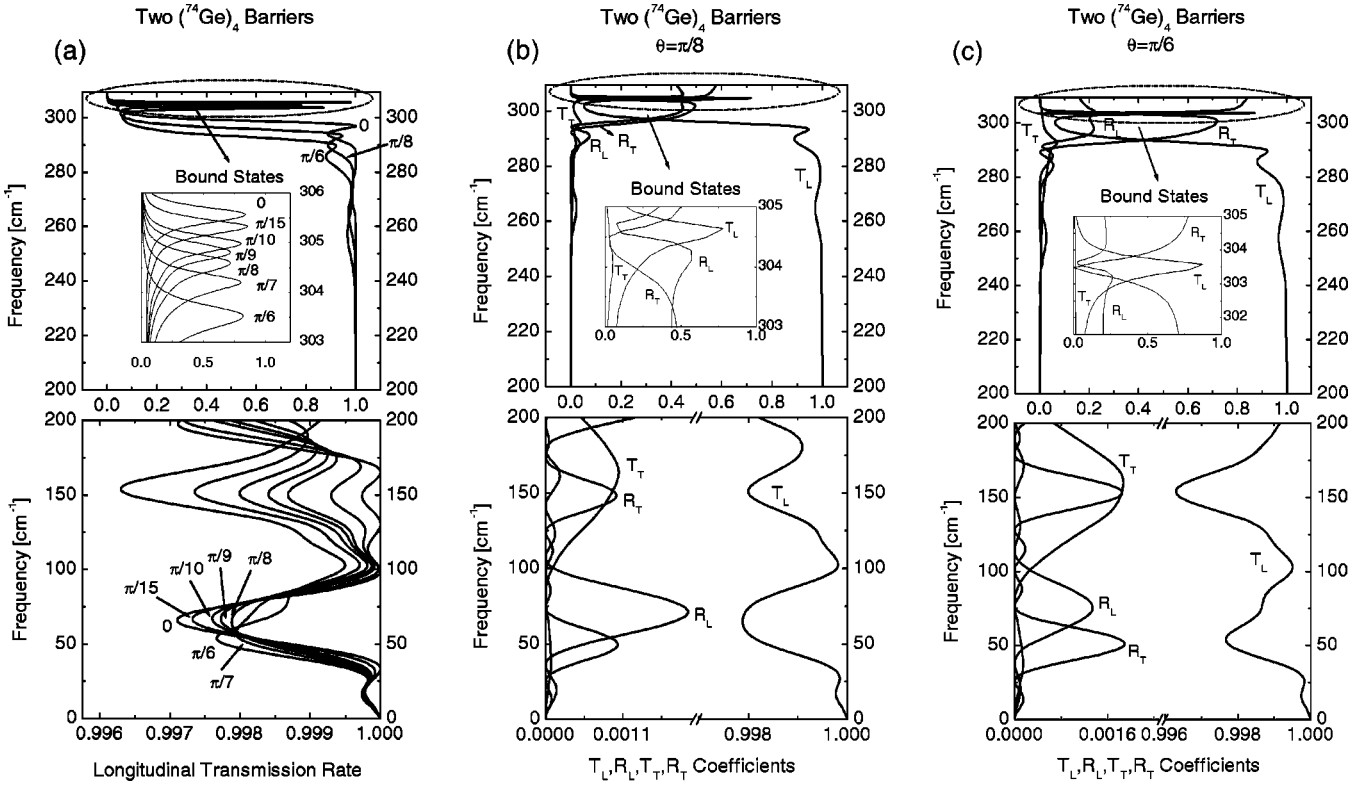

FIG. 4. Transmission and reflection coefficients vs frequency (in cm^{-1}) for the double-barrier structure (bulk ^{70}Ge-(^{74}Ge)$_4$-(^{70}Ge)$_4$-(^{74}Ge)$_4$-bulk ^{70}Ge). (a) Transmission coefficient for L phonons (T_L) for the angles of incidence $\theta = 0$, $\pi/15$, $\pi/10$, $\pi/9$, $\pi/8$, $\pi/7$, and $\pi/6$. The coefficients T_L, T_T, R_L, and R_T for the angles (b) $\theta = \pi/8$ and (c) $\theta = \pi/6$ are also plotted. See the text for details.

comes larger, the deviation tends to zero.[5] In Fig. 3 the B SL is replaced by 80 periods of bulk ^{70}Ge. The resonance is also well explained by the above conditions.

We shall now study in detail the coupling between L and T modes through the phonon tunneling. We consider the incidence from the left of a longitudinal phonon with wave vector tilted by an angle θ with respect to the longitudinal wavevector of the substrate in the z direction (k_L). In order to obtain information of each mode, the L and T transmission and reflection coefficients (26–30) are evaluated.

In Fig. 4(a) the transmission coefficient for optical and acoustic longitudinal phonons (T_L) for a double-barrier structure [bulk ^{70}Ge$-$(^{74}Ge)$_4-$(^{70}Ge)$_4-$(^{74}Ge)$_4-$bulk ^{70}Ge] is plotted for incidence angles equal to $\theta = 0$, $\pi/15$, $\pi/10$, $\pi/9$, $\pi/8$, $\pi/7$, and $\pi/6$. Increasing the angle θ—which corresponds to a larger transverse wave vector κ—the peaks and dips shift to lower (larger) frequencies for the optical (acoustic) modes. This is the expected behavior when compared with the trends in the dispersion relation for $\kappa \neq 0$. The phonon modes are greatly influenced by the bulk dispersion relations. We checked this statement numerically, but do not show the explicit results because they are equivalent to the ones here discussed. Examples are found in the calculations for Si/Ge heterostructures[26] and the results for mixed polar-nonpolar systems.[27] The reason for this behavior is that the oscillations with longest wavelength do not satisfy the change in the symmetry in the growth direction (the cubic symmetry of the host material is replaced for the orthorhombic symmetry of the SL). Oscillations in the highest peaks and dips are observed (see the inset for optical bound states, and the second dip for acoustic phonons). Similarly, the relative values of the different coefficients change with the incidence angle [compare the R_L and R_T coefficients in Figs. 4(b) and 4(c)]. This means that the values of the coefficients characterizing the transverse component of the mode do not change monotonically, as could be expected from the shifting effect. By increasing the incidence angle we extend the distance the phonon needs to travel through the heterostructure, and the interference profile changes. This effect competes with the increase of the transverse component of the phonon mode for larger angles. An oscillatory behavior was predicted theoretically for the Ge eigenfrequencies in Si/Ge SL's as the SL period is increased,[28] and an oscillatory behavior for the transmission rate as a function of the number of monolayers was found in Ref. 29 by approximating the 3D tunneling problem as a 1D one. In Ref. 28 it was explained that in real structures the presence of Ge_xSi_{1-x} alloys in the interface destroys the interference effects, and it is not possible to observe the oscillations. We suppose that isotopic SL's are excellent candidates in which to observe the aforementioned features, for the following reasons. First, the interfaces have great quality because the compound materials are very similar. Second, the transmission peaks and dips are very broad, and easy to detect, due to the high dispersive character of the phonon modes.

For acoustic phonons T_L is closer to unity than for optical

phonons. This is a consequence of the fact that acoustic modes are more extended through the whole structure, and shows that L and T modes are less coupled than for optical phonons.

V. THERMAL CONDUCTIVITY

Hyldgaard and Mahan[17] and Tamura *et al.*[19] found, employing a Debye-like model, that the reduction in the SL thermal conductivity at high temperature with respect to the bulk one is an order of magnitude for Si/Ge structures, and about three times that for a GaAs/AlAs SL. The same quantitative behavior was found with more realistic models in Refs. 20 and 21. The differences between these two cases correspond to the relative phonon band gap width of the host materials. In the Si/Ge system the modes are in general more confined; also, the phonon branches are less dispersive, consequently with smaller average group velocities than in the GaAs/AlAs system. For an extensive discussion, see Ref. 18. Due to the overlapping of bulk phonon bands, the reduction corresponding to the isotopic SL is expected to be more modest than in the two former cases. But the point that we will address is the influence of the optical phonons, not considered by other authors (except, very recently, for the smaller influence for Si/Ge structures discussed in Ref. 20). The contribution of optical phonons is expected to be important at high temperatures (as commented upon in Sec. I) in the latter system. In Fig. 1 we observe that the dispersive character of the optical modes is comparable to that of the acoustic ones. The thermal conductivity of bulk germanium with different isotopic compositions was studied intensively in Ref. 30.

As in Ref. 17 we consider the ratio of the superlattice perpendicular thermal conductivity $\tilde{\kappa}_{SL}$ to phonon relaxation time τ_{SL} (assuming it is independent of the frequency) given by

$$\frac{\tilde{\kappa}_{SL}}{\tau_{SL}} = \sum_{\lambda} \int \frac{d^2\kappa}{(2\pi)^2} \int_{-\pi/d}^{\pi/d} \frac{dq}{2\pi} \hbar \omega_{\lambda} \left(\frac{\partial \omega_{\lambda}}{\partial q} \right)^2 \frac{dN}{dT}, \quad (34)$$

where λ is the set of labels of the states, and $N=N(T)$ is the Bose-Einstein distribution function at temperature T.

In Fig. 5 we show the calculated ratio of the perpendicular thermal conductivity to the phonon relaxation time as a function of temperature for the $(^{70}\mathrm{Ge})_4$-$(^{74}\mathrm{Ge})_4$ SL. For the sake of comparison we also include this magnitude for the bulk ^{70}Ge (dashed line). We describe the phonons in any direction of reciprocal space by the simple relations obtained from Eq. (11) (the parameters are fitted to the entire Brillouin zone of the host material). We represent the contribution of acoustic phonons by a dotted line, and that of both acoustic and optical phonons by a solid line. The same order of magnitude and trends as in Refs. 17 and 19–21 are found. The reduction of the thermal conductivity in the SL with respect to the bulk is lower (about 3/2) than in the Si/Ge and GaAs/AlAs systems, as commented upon above. We expect a small overestimate due to the approximation employed, i.e., neglecting the gaps in the SL dispersion relation. Finally we observe

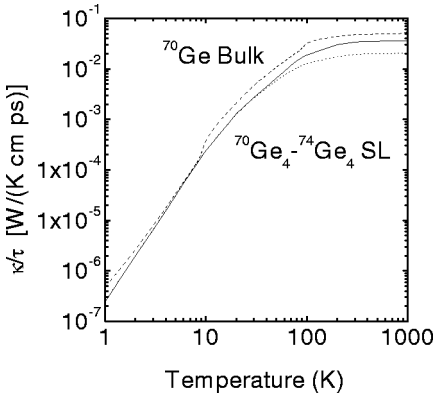

FIG. 5. Ratio of the perpendicular thermal conductivity $\tilde{\kappa}_{SL}$ to phonon relaxation time τ_{SL} as a function of temperature. For the $(^{70}\mathrm{Ge})_4$-$(^{74}\mathrm{Ge})_4$ SL, we represent the contribution of the acoustic modes by a dotted line, and that of both acoustic and optical modes by a solid line. The values for the bulk ^{70}Ge are represented by dashed lines.

that the contribution of the optical phonons at high T is about the 5/9 of the acoustic phonons, and in principle should be considered in other studies.

VI. CONCLUSIONS

We have presented a recently developed phenomenological long-wavelength model as a general approach which describes (with an appropriate choice of the parameters) both acoustic and nonpolar optical phonons in semiconductor heterostructures. We have shown the necessity of considering together acoustic and optical phonons to obtain the best description of all modes. From a postulated Hamiltonian density, the equations of motion and a continuity equation for the energy density are derived straightforwardly. The transmission and reflection coefficients are defined rigorously. For cubic symmetry we have shown that there is no interference between the energy density fluxes of L and T modes. Our calculations are valid while the conditions either $\omega_L = \omega_T$ or $\boldsymbol{\kappa}=0$ hold, i.e., it is an exact result for unstrained material and an approximation for strained ones.

We have calculated the transmission coefficients in structures made up by nonpolar materials. In particular, we have presented results for some isotopic Ge finite SL's. From the analysis of isotopic and Si/Ge (Ref. 24) superlattices, we can conclude the following rules: (1) Resonance peaks in the transmission rate characterize the confined modes. The height of the peak depends on the penetrability of the mode in the adjacent layer, e.g., in the $(\mathrm{Si})_4$-$(\mathrm{Ge})_4$ SL only the Si mode confined at the interface have a transmission rate close to unity, and the other Si modes have a vanishing small maximum value of T_L.[11,24] (2) The extended modes have thick peaks which are limited by dips. (3) The broader peaks are related to more dispersive bands, and consequently to a greater phonon group velocity. (4) In a multiple-superlattice system specific resonance conditions following from the additional superperiodicity are also found. (5) For oblique directions $(\theta, \boldsymbol{\kappa} \neq 0)$ the phonons are greatly influenced by the behavior of the bulk dispersion relations.

In the study of the phonon tunneling, for the case of oblique incidence, oscillations in the relative contribution of the different coefficients for a variation of the incidence angle are found. We expect that this behavior could be detected experimentally in the isotopic SL's.

In all the cases studied the infinite SL is recovered as the number of periods increases. In practice, about 20 periods are sufficient to obtain the features of the infinite case. In spite of the long-wavelength nature of the model employed, we have obtained good results for large values of the wave vector.

For isotopic SL's it is possible to obtain, for each phonon band, explicit relations between the phonon frequency and phonon wave vector for the entire Brillouin zone. Based on these results we conclude that in this system the contribution of optical phonons to the thermal conductivity should be taken into account.

[1] B. Jusserand and M. Cardona, *in Light Scattering in Solids V*, edited by M. Cardona and G. Güntherodt (Springer-Verlag, Heidelberg, 1989).

[2] R. Tsu and S.S. Jha, Appl. Phys. Lett. **20**, 16 (1972); A.S. Barker, Jr. J.L. Merz, and A.C. Gossard, Phys. Rev. B **17**, 3181 (1978).

[3] E. Molinari, A. Fasolino, and K. Kunc, Superlattices Microstruct. **2**, 397 (1986).

[4] S. Tamura, D.C. Hurley, and J.P. Wolfe, Phys. Rev. B **38**, 1427 (1988), and references therein.

[5] S. Mizuno and S. Tamura, Phys. Rev. B **45**, 734 (1992); Jpn. J. Appl. Phys. **32**, 2206 (1993).

[6] B.K. Ridley, Phys. Rev. B **49**, 17 253 (1994).

[7] C. Trallero-Giner, F. García-Moliner, V.R. Velasco, and M. Cardona, Phys. Rev. B **45**, 11 944 (1992).

[8] F. Comas, R. Pérez-Alvarez, C. Trallero-Giner, and M. Cardona, Superlattices Microstruct. **14**, 95 (1993); R. Pérez-Alvarez, V.R. Velasco, and F. García-Moliner, Phys. Scr. **51**, 526 (1995).

[9] C. Trallero-Giner, R. Pérez-Alvarez, and F. García-Moliner *Long Wave Polar Modes in Semiconductor Heterostructures*, (Pergamon/Elsevier Science, London 1998).

[10] A.J. Shields, M. Cardona, and K. Eberl, Phys. Rev. Lett. **72**, 412 (1994); C. Trallero-Giner, A. Debernardi, M. Cardona, E. Menéndez-Proupin, and A.I. Ekimov, Phys. Rev. B **57**, 4664 (1998).

[11] F. de León-Pérez and R. Pérez-Alvarez, Phys. Rev. B **61**, 4820 (2000).

[12] E.B. Christoffel, Annu. Mater. Pura Appl. **8**, 193 (1877); see also A.G. Every, Phys. Rev. Lett. **42**, 1065 (1979), Phys. Rev. B **22**, 1746 (1980).

[13] V. Narayamurti, H.L. Störmer, M.A. Chin, A.C. Gossard, and W. Wiegmann, Phys. Rev. Lett. **43**, 2012 (1979); G.A. Northrop and J.P. Wolfe, Phys. Rev. B **22**, 6196 (1980); J.P. Wolfe, Phys. Today **33**(12), 44 (1980); in *PHONONS 89*, edited by S. Hunklinger, W. Ludwing, and G. Weiss (World Scientific, Singapore, 1989), p. 1335; in *Festkörperprobleme/Advances in Solid State Physics*, edited by U. Rössler (Vieweg, Braunschweig, 1989), Vol. 29, p. 75; Phys. Today **48**(9), 34 (1995); R.L. Weaver, M.R. Hauser, and J.P. Wolfe, Z. Phys. B: Condens. Matter **90**, 27 (1993).

[14] T. Yao, Appl. Phys. Lett. **51**, 1798 (1987); X.Y. Yu, G. Chen, A. Verma, and J.S. Smith, *ibid.* **67**, 3554 (1995).

[15] W.S. Capinski, M. Cardona, D.S. Katzer, H.J. Maris, K. Ploog, and T. Ruf, Physica B **263&264**, 530 (1999); W.S. Capinski, H.J. Maris, T. Ruf, M. Cardona, K. Ploog, and D.S. Katzer, Phys. Rev. B **59**, 8105 (1999); S.M. Lee, D.G. Cahill, and R. Venkatasubramanian, Appl. Phys. Lett. **70**, 2957 (1997).

[16] L.D. Hicks and M.S. Dresselhaus, Phys. Rev. B **47**, 12 727 (1993); M.A. Weilert, M.E. Msall, J.P. Wolfe, and A.C. Anderson, Z. Phys. B: Condens. Matter **91**, 179 (1993); M.A. Weilert, M.E. Msall, A.C. Anderson, and J.P. Wolfe, Phys. Rev. Lett. **71**, 735 (1993); G.D. Mahan and H.B. Lyon, Jr., J. Appl. Phys. **76**, 1899 (1994); J.O. Sofo and G.D. Mahan, Appl. Phys. Lett. **65**, 2690 (1994); D.A. Broido and T.L. Reinecke, Phys. Rev. B **51**, 13 797 (1995).

[17] P. Hyldgaard and G.D. Mahan, Phys. Rev. B **56**, 10 754 (1997).

[18] M.V. Simkin and G.D. Mahan, Phys. Rev. Lett. **84**, 927 (2000).

[19] S. Tamura, Y. Tanaka, and H.J. Maris, Phys. Rev. B **60**, 2627 (1999).

[20] A.A. Kiselev, K.W. Kim, and M.A. Stroscio, Phys. Rev. B **62**, 6896 (2000).

[21] W.E. Bies, R.J. Radtke, and H. Ehrenreich, J. Appl. Phys. **88**, 1498 (2000).

[22] M. Cardona, in *Festkörperprobleme/Advances in Solid State Physics*, edited by R. Helbig (Vieweg, Braunschweig, 1994), Vol. 34, p. 35; E. E. Haller, J. Appl. Phys. **77**, 2857 (1995); H.D. Fuchs, P. Molinàs-Mata, and M. Cardona, Superlattices Microstruct. **13**, 447 (1993); J. Spitzer, T. Ruf, M. Cardona, W. Dondl, R. Schorer, G. Abstreiter, and E.E. Haller, Phys. Rev. Lett. **72**, 156 (1994); J. Spitzer, Ph.D. thesis, University of Stuttgart, 1994; M. Cardona, P. Etchegoin, H.D. Fuchs, and P. Molinàs-Mata, J. Phys.: Condens. Matter **5**, A61 (1993).

[23] R. Pérez-Alvarez and F. de León-Pérez, Phys. Scr. **58**, 525 (1998).

[24] F. de León-Pérez and R. Pérez-Alvarez, in *Proceedings of the Latin-American Congress of Surface Science and its Applications*, edited by O. Melo and I. Hernández (World Scientific, Singapore, 2000), Sec. p. 305.

[25] G. Nilsson and G. Nelin, Phys. Rev. B **3**, 364 (1971).

[26] F. de León-Pérez and R. Pérez-Alvarez, in *Proceedings of the 27th Meeting of the Spanish Phys. Society, Valencia, 20-24 Sept 1999*; edited by M. V. Castillo, A. Ferrer and E. Higón (Universidad de Valencia, Valencia, 1999), Vol. II, pp. 440 and 441.

[27] F. de León-Pérez and R. Pérez-Alvarez, Phys. Rev. B **62**, 9915 (2000).

[28] F. Cerdeira, M.I. Alonso, D. Niles, M. Garriga, M. Cardona, E. Kasper, and H. Kibbel, Phys. Rev. B **40**, 1361 (1989); O. Brafman, M.A. Araújo Silva, F. Cerdeira, R. Manor, and J.C. Bean, *ibid.* **51**, 17 800 (1995); M.A. Araújo Silva, E. Ribeiro, P.A. Schultz, F. Cerdeira, and J.C. Bean, *ibid.* **53**, 15 871 (1996).

[29] H. Kato and S. Tamura, J. Phys.: Condens. Matter **9**, 6791 (1997).

[30] M. Asen-Palmer, K. Bartkowski, E. Gmelin, M. Cardona, A.P. Zhernov, A.V. Inyushkin, A. Taldenkov, V.I. Ozhogin, K.M. Itoh, and E.E. Haller, Phys. Rev. B **56**, 9431 (1997).